JOURNAL OF ENGINEERING AND EARTH SCIENCES

JEES ISSN: 1897-8680

JEES 2024

VOLUME 17 ISSUE NO 1

PAGE 33 - 42

PRE AND POST - CORROSION MECHANICAL PROPERTIES OF COPPER ALLOYED GREY CAST IRON

[1*]Kutelu, B. J., [2]Oluyori, R. T., and [3]Omoyeni, D. O.

[1,3] Department of Mineral and Petroleum Resources Engineering Technology, The Federal Polytechnic Ado - Ekiti

[2] Department of Metallurgical and Materials Engineering, Kogi State Polytechnic, Lokoja, Kogi State

*Corresponding author email: rinwa2006@yahoo.com

ABSTRACT

In this study, the influence of varied copper additions on the microstructures and mechanical properties of grey cast iron (GCI) before and after corrosion was investigated. The chemical compositions of the samples were determined using an optical spectrometry - AR 4 30 metal analyzer. The samples were machined to tensile and hardness test specimens following ASTM E8-08 and ASTM E384-11 respectively, and tested on an INSTRON tensile testing machine and scale C Rockwell hardness tester for tensile and hardness measurements respectively. An optical metallurgical microscope Olympus Model GX51 with a camera attached was used for microstructural examination. The potentiodynamic polarization technique (Autolab PGSTAT 204N) was used for the corrosion test. The results showed that the carbon equivalent values (CEVs) of both the control and copper alloyed samples were Hypo-eutectic GCI. The microstructures of all the samples before and after corrosion were heterogeneous. Graphite flakes of the control sample were thick and sparsely distributed in the ferritic matrix relative to the copper-alloyed samples, which were densely distributed within the ferritic matrix. The highest values for tensile strength and hardness before and after corrosion of 289 MPa and 20.96 HRC respectively, and the corresponding post-corrosion tensile values were 286 MPa and 20.74 HRC respectively, and the values were revealed by the sample with 1.6 wt. %Cu addition. The corrosion-resistant characteristics of the copper alloyed samples were superior to the control sample. Corrosion rates of 0.06752 mmpy and 0.09593 mmpy were revealed by samples with 1.6 wt. % Cu and 1.8 wt. % Cu addition respectively, and hence 1.6 wt. % Cu is the optimum copper requirement.

KEYWORDS: Microstructure; corrosion; graphite flakes; heterogeneous; ferritic matrix; pearlitic-ferritic matrix

INTRODUCTION

Grey cast iron (GCI) is a low-cost product, accounting for approximately 70% of global ferrous alloy castings, it is an iron-carbon-silicon alloy, with other elements, including manganese, phosphorous, sulphur, and aluminium in trace quantities (Sherrif et al., 2017; Koch et al., 2016; Agunsoye et al., 2014). GCI is characterized by excellent castability, good conductivity, relatively low melting temperature, high damping capacity, and it is used in diverse areas of engineering applications construction material, and it is the traditional material in automotive castings for the engine block and brake component (Seikh et al., 2019; Sherrif et al., 2017; Vadiraj et al., 2014; Sefiu et al, 2014). In recent, the use of GCI has been challenged by compacted grey iron (CGI) and aluminium due to superior mechanical properties and weight requirements respectively. This is despite its relative production simplicity and low cost of production (Sherrif et al., 2019; Agunsoye et al., 2014; Seidu, 2014). GCI properties are influenced by phase, size, amount, and method of graphite distribution. Therefore, the issues of GCI properties (mechanical and corrosion) have been largely addressed by microstructure modification through alloying (Behnam et al., 2010; Rana et al., 2001), and it has been revealed that single-phase microstructures such austenite, ferrite, and martensite outperformed two-phase mixes like tempered martensite, bainite and pearlite in corrosive conditions (Rundman et al., 2005; Lunarska, 1996).

Corrosion is a huge problem for engineering structures, accounting for about 3.4% of global gross domestic product (GDP) (Seikh et al., 2017; Koch et al., 2016). GCI is more susceptible to corrosion attack relative to steel due to high carbon content, graphite flakes, and iron matrix (Asadi & Melchers, 2017). The service life of GCI has been improved substantially through copper and nickel alloying. However, the use of the former has gained appreciable acceptance due to its low cost (Hector et al., 2024; Fateh et al., 2020). Copper is characteristically a noble metal, providing good corrosion resistance to a number of environments, including the atmosphere and some chemical environments, forming a protective passive (oxide) film or non-conductive layer of corrosion products on its surface (Fatch et al., 2020; Stan et al., 2010). (Hector et al., 2024).

Copper exhibits moderate hardness and ductility, and it is a mild graphitizer, copper promotes, refines, and stabilizes pearlite and increases the number of eutectic cells, decreases the size of the cell and lump size when added to GCI (Sarkar et al., 2017; Xu et al., 2005), and according to Bates, (1997) copper addition to GCI up to 0.5% increased yield and ultimate strengths, while higher concentrations produced almost negligible effect due to the resulting fully pearlitic base iron. The presence of copper with 99.9% purity in grey cast iron melt prevented the formation of cementite, and the addition of 1 to 3.5 wt.% copper altered the composition and mechanical properties of cast iron, which resulted in improved wear resistance (Agunsoye et al., 2014). Copper has shown a greater impact on ferritic or ferritic plus pearlite irons, and as copper content rises, tensile strength and hardness properties are increased (Pluphrach, 2010). Seidu et al. (2015) assessed the effect of 3.0 wt.%, 2.5 wt.%,2.0 wt.%, and 1.5 wt.% copper on corrosion behavior of grey cast iron, and revealed that samples with 2.0 wt.% and 1.5 wt.% of copper gave excellent resistance in salt and basic environment, while good corrosion resistance was revealed by the samples with 3.0 wt.%, 2.5 wt.% copper. However, the corrosion resistance characteristics of all the samples were poor in an acid environment. Upadhyay and Saxena (2020) reviewed the effect of molybdenum (Mo) and copper (Cu) addition in grey cast iron and reported that with an increased percentage of Mo and Cu, the tensile strength and hardness of the grey cast iron were increased, while the impact energy was decreased. But beyond a certain amount of Mo and Cu additions, significant effects on these properties were not noticed.

Hector et al. (2024) investigated the effect of copper and nickel contents on corrosion mechanisms in the ferrite matrix of grey cast iron under a stimulated matrix environment and reported that addition of copper led to an increase in goethite phase in the long–term, while addition of nickel contributed to the formation of oxyhydroxide like lepidocrocite, characterized by a negative charge, which did not favour interaction of chloride ion, and hence delay occurrence of corrosion process. Also, samples with combined copper and nickel contents did not reveal the effect of synergy, as the alloying elements were practically independent. The short-term decrease in corroded thickness was attributed to nickel contribution by the formation of oxyhydroxide like lepidocrocite, while the goethite phase, which appeared in the long-term, and increased corrosion resistance was attributed to copper content. The efforts of the past researchers so far have informed the need to further work on the investigation of microstructure and mechanical properties of grey cast iron before and after corrosion, it is aimed at evaluating the effect of corrosion with the objective of determining optimum copper requirement for enhance service life of the material in chloride environment.

MATERIALS AND METHOD

Materials

Materials used for the study are Auto parts scraps, ferrosilicon (FeSi), limestone, and copper, and they are depicted in Plate 1A, B, C, and D respectively.

Plate 1(A-D). Auto parts scrap, ferrosilicon (FeSi), limestone, and copper respectively used for grey cast iron sample production

Methods

Sample preparation and casting

The greensand mould was used, and it was prepared by mixing bentonite and coal dust with an appropriate amount of water. The wooden rectangular pattern of length 50 mm and breadth 30 mm pattern was used shrinkage, machining, draft, wrapping, and distortion allowance were ensured. The auto parts scraps were broken into smaller sizes, using sledge hammer to allow for free passage through the charging sprout of a 50kg rotary furnace, thereby protecting the lining from eroding, and enhancing rapid melting and reduction in slag content in the melt by controlling the number of charges (Sherrif et al., 2019; Seidu, 2014).

The furnace was preheated for about 1 hour before charging to allow for effective melting and achieving a uniform melting rate (Sherrif et al., 2019; Seidu, 2014). The charge was heated to 1,485°C and at this temperature, the charge was melted completely and ready for tapping into the ladle, which had been preheated. The temperature of the melt was monitored at regular intervals, using an optical pyrometer. When tapping, the melts were treated with copper and FeSi alloy inoculant (78% Si, 0.21% Al, Fe-bal and particle size in the range of 0.5 to 1.5 mm. The first melt, which is the control sample was treated with 0.3wt.% FeSi inoculant. While the second, third, and fourth melts were treated with 0.3wt.% FeSi and 1.4wt. %, 1.4wt. % and 1.4wt. % copper respectively, and during tapping, the slag, floating on top of the melt was removed with the aid of a mild steel rod before pouring to prevent slag inclusions in the casting. The melt was left for a day in the mould to avoid any hot shaking effects on the solid-state solidification while ensuring gradual transformation into a solid cast at room temperature.

The castings were knocked out after the melt had completely solidified. The cope was separated from the drag by rigorous shaking and the cast produced was carefully removed by knocking out from inside the drag. The successful cast came out of the mould with unwanted protrusions including the gating horns and channel marks. Then all the unwanted body attachments were cleaned off by cutting and wire brushing respectively.

Chemical analysis

The chemical composition of the castings (control sample and copper alloyed samples) was determined, using Optical emission spectrometry (AR 4 30 metal analyzer).

Microstructure

Surfaces of metallographic samples were ground, using a laboratory grinding machine with sets of emery papers starting from the coarsest one to the finest. Emery papers of grades 60, 120, 240, 320, 400, 800, and 1200 microns were used. As the emery papers were changed from one to the

other, the samples were turned through an angle of 90 to remove the scratches sustained from the previous grinding until a scratch-free surface was obtained. After grinding, the samples were polished using a laboratory polishing machine to give a mirror-like surface using billiard cloth.

The billiard cloth consists of abrasive particles that are not firmly fixed but suspended in a liquid among the fibres of the cloth. Diamond paste of different microns (6m,3m,1m) was applied on the billiard cloth and the samples were polished by holding it with less pressure against the rotating disc until a mirror-like surface was obtained. The samples were examined under a metallurgical microscope at a magnification of 400.

The micrographs were etched with nital (3% nitric acid and 97% ethanol) for the required time by applying the etchant with cotton wool. The etching action was stopped by placing the samples under a stream of water. Then the samples were cleaned with alcohol, dried well, and ensured that the polished and etched surfaces were not altered (especially by finger or cloth).

Hardness test

Hardness specimens with dimensions 20 mm length, 20 mm breadth, and 4.5 mm thickness (Figure 2) were prepared based on ASTM E384-11 (2011) standard, Universal Rockwell hardness tester model 8187LKV for hardness measurement on C-Scale by placing the specimens on the anvil, which was moved up until it came in contact with the diamond cone indenter, the dial gauge was set to zero using a minor load of 10 kgf, which was followed by a major load of 150 kgf. Three indentations were made with a gap of about 3 mm in-between and the average values were recorded.

Mechanical testing

Tensile test

The tensile test samples were machined to standard tensile specimens based on ASTM E8-08 (2008) (Figure 1). And mounted at its ends onto the holding grips of the testing apparatus. They were then tensioned till a fracture occurred, and tensile readings were recorded.

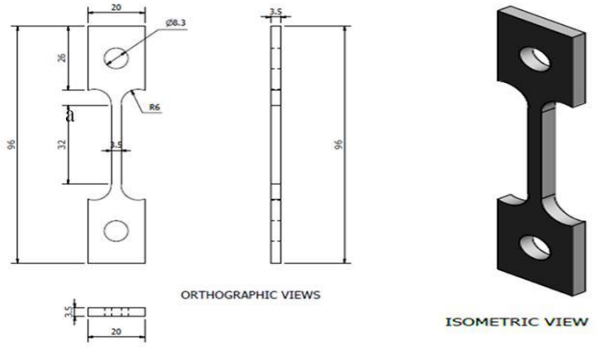

Figure 1: Tensile test specimen

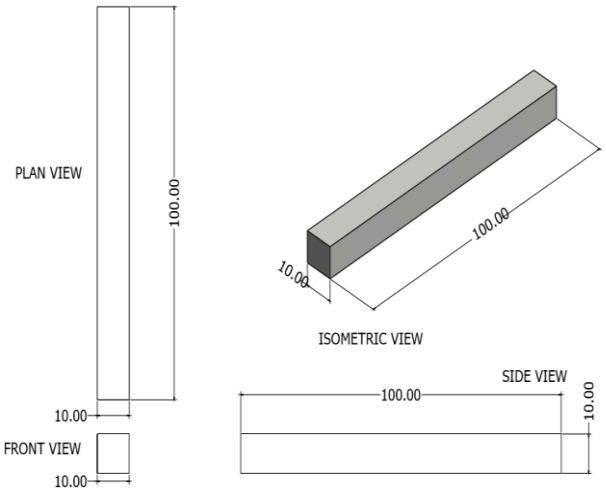

Figure 2: Hardness test specimen

Electrochemical studies

The potentiodynamic polarization technique was used for the study. Corrosion coupons of size 20 mm in length, 10 mm in breadth, and 4.5 mm in thickness were mounted in resin and connected with a flexible wire. The mounted coupons were then ground, polished, cleaned, and rinsed

properly following ASTM G36 standard. A three-electrode electrochemical system was set up. Saturated silver/silver chloride was used as the reference electrode, platinum as the counter/ auxiliary electrode, and the coupons as the working electrode. An area of 1cm^2 of the coupons was exposed to an aqueous solution of 0.1M HCl)., and corrosion data were recorded, using a computer-based data logging system (Auto lab PGSTAT 204N), which was piloted by NOVA software for corrosion analysis. The experiments were performed according to ASTM G3-14 at room (25^{o}C) temperature.

RESULT AND DISCUSSION

Chemical analysis

From the chemical analysis results (Table 1), the control sample and copper alloyed samples are comprised mainly of carbon and silicon. While the other elements, comprising manganese, phosphorous, and sulphur occur in trace amounts. The range of silicon contents of the samples (control and copper alloyed samples) indicates that they are grey-cast irons because, at these high silicon levels, graphite formation is favoured against carbide formation (ASTM A247, 2006; Davis, 2012). This is suggestive from the calculated carbon equivalent values (CEVs) of both the control sample - 3.15 wt. %, and copper alloyed samples (1.4 wt.%) – 3.01 wt.%, (1.8 wt. %) – 3.08 wt. %, 2.2 wt. % - 3.17 wt. %; that they are hypo-eutectic grey cast iron (Lina, 2018; Seidu, 2014; Deckar, 2005).

Table 1. Chemical analysis of the grey cast iron samples

Grey cast iron	Chemical Composition wt.%						CE (wt. %)	Mn/S	(Mn)x (S)
	C	Si	Mn	P	S	Al			
Control	3.08	2.45	0.234	0.088	0.135	0.0010	3.15	1.73	0.032
1.4wt%Cualloy	3.01	2.93	0.220	0.069	0.143	0.0076	3.10	1.54	0.031
1.8wt%Cualloy	3.10	2.98	0.201	0.060	0.140	0.0087	3.08	1.43	0.028
2.2wt%Cualloy	3.03	2.98	0.101	0.071	0.149	0.0098	3.17	0.68	0.015

Pre corrosion microstructures

The pre-corrosion microstructure of the control GCI sample and copper alloyed GCI samples, shown in Plate 2 (a-d) respectively are heterogeneous, comprising graphite flakes of varying sizes, and pearlite and ferrite of varied volume fractions. The thick and sparse graphite flakes in the ferrite matrix, characterizing the microstructure of the control sample were due to low graphitization that resulted from the absence of copper, because copper promotes graphitization (Riposan et al., 2010). Conversely, the somewhat thin graphite of different morphologies in the pearlite matrix, characterizing microstructures of copper was expected, and resulted from copper addition, because copper promotes graphitization, refines, and stabilizes pearlite (Sheriff et al., 2017; Seidu, 2014; Riposan et al., 2010; Stan et al., 2010).

Plate 1: Pre-corrosion microstructures of (a) 0.0wt.%Cu (control) sample and (b) 1.4wt. %, (c)1.6wt. % and (d) 1.8wt.% copper alloyed samples

Pre-corrosion tensile and hardness properties

The superior tensile strength and hardness properties of the copper alloyed samples relative to the control sample shown in Figure 1 and Figure 2 can be hinged on phases, size, amount, and distribution of graphite within the samples' microstructures, which were influenced by copper addition. In congruence, Agunsoye et al. (2014) have revealed that copper addition to grey cast alters graphite shape and distribution, with concomitant improvement in tensile strength and hardness properties. The highest tensile strength value of 289 MPa and hardness value of 20.96 HRC were revealed by the sample with 1.6 wt. % Cu addition, which represents the optimum copper requirement was due to the higher pearlite-to-ferrite ratio and increased presence of more small size of graphite flakes within the microstructure (Upadhyay & Saxena 2020; Agunsoye et al., 2014; Adedayo, 2013; Bates, 1984). Since copper promotes graphitization, a reduced tensile strength value of 286 MPa and hardness values of 20.74 HRC shown by the sample with the subsequent addition of copper (1.8 w. %) was not least expected, and was due to decreased volume fraction of pearlite and increased volume fraction of graphite.

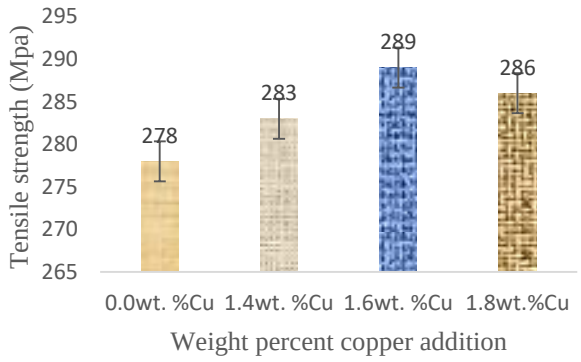

Figure 1: Pre-corrosion tensile strength property of the samples at varied percent copper addition

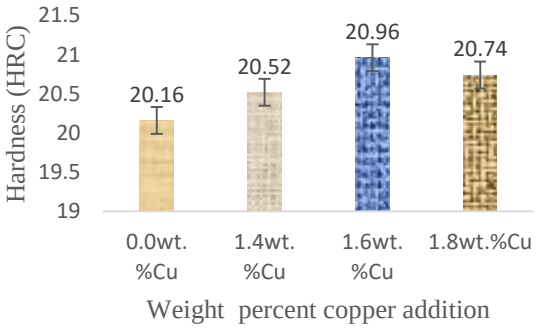

Figure 2: Pre-corrosion hardness property of the of the samples at varied percent copper addition

Electrochemical studies

High corrosion-resistant characteristics shown by the copper alloyed samples relative to the control sample (Figure 3) resulted from the presence of copper, which is a characteristic noble metal, providing good corrosion resistance to a number of environments by forming a protective passive (oxide) film or non-conductive layer of corrosion products (Fatch et al., 2020; Akimov et al., 1981). Due to the microstructural heterogeneity of grey cast iron, the propensity for cathodic and anodic site formation was high. And the consequent least anodic reaction (increase shift to a more positive potential), with a corrosion rate of 0.06752 mmpy, is shown by the sample with 1.6 wt. % Cu addition, which represents the optimum copper requirement was due to the conjoint effect of higher pearlite-to-ferrite volume fraction and relatively fine microstructure (Seikh et al., 2016). The increased shift to a less positive potential (i.e. more anodic or increased corrosion kinetics) with an increased corrosion rate of 0.09593 mmpy, shown by the sample with the subsequent addition of copper to 1.8 wt. % was indicative of the fact that beyond 1.6 wt. % copper addition, further addition copper held no significant positive effect on the corrosion-resistant characteristics, but rather

more graphitization, which in effect favours graphitic corrosion (Hector et al., 2024).

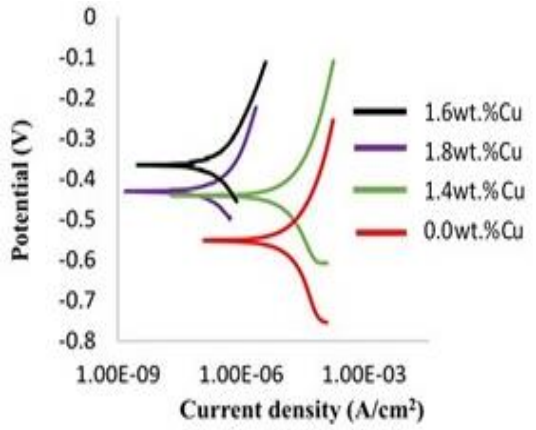

Figure 3: Polarization curves of the samples at varied weight percent copper addition

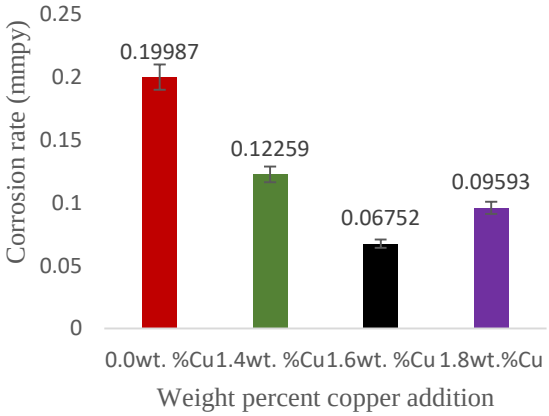

Figure 4: Corrosion rate characteristics of the samples at varied weight percent copper addition

Post corrosion microstructures

In terms of characteristic features, the microstructures of the samples after corrosion are similar to the microstructures of the samples before corrosion. Generally, the corroded microstructures are composed of graphite flakes with varied volume fractions of ferrite and pearlite (Melchers, 2013; Tel'manova et al., 2012). However, in terms of corrosion attack, the microstructures are variably attacked due to composition differential (refer to Table 1). The more obvious corrosion susceptibility of the control sample was due to the absence of a protective passive (oxide) film or non-conductive layer of corrosion products from copper addition (Fatch et al., 2020; Hsu et al., 2012).

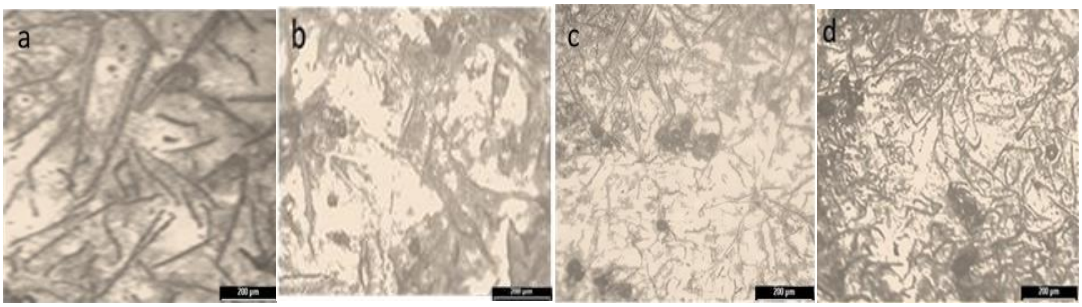

Plate 2: Post-corrosion microstructures of (a) 0.0wt.%Cu (control) sample and (b) 1.4wt. %, (c)1.6wt. % and (d) 1.8wt.% copper inoculated samples in 0.5 HCl

Post-corrosion tensile and hardness properties

Similar to the post-corrosion results, the tensile strength and hardness properties of copper alloyed samples were superior relative to the corresponding tensile strength and hardness properties of the control sample (refer to Figure 5 and Figure 6). In comparison, the obvious inferior tensile strength and hardness properties of the samples after corrosion than before corrosion was expected and it is in concordance with findings of the past researchers (Asadi & Melchers, 2017; Saliu et al., 2015; Hsu.,& Chen, 2010; Lunarska, 1996), It is well known that corrosion attack presents deleterious effects on

properties of metals and corrosion of GCI is exacerbated by high carbon content, graphite flakes and iron matrix (Asadi & Melchers, 2017; Ruscak., & Perng. 1995). Highest tensile strength value of 279 MPa and hardness value of 20.29 HRC as shown by the sample with 1.6 wt. %Cu addition was due to more volume fraction of pearlite relative to ferrite because the former has been associated with corrosion resistance. In addition, the observed relative graphite flake size reduction was contributory. The subsequent addition of 1.8 wt. % copper, and the resulting reduction in tensile strength (286 MPa) and hardness (20.74 HRC) may be due to increased graphitic corrosion that resulted from more graphitization. Hence, graphitization is a distinguishing feature of the GCI deterioration properties.

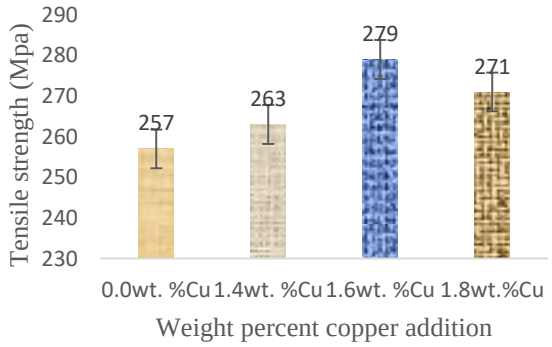

Figure 5: Post-corrosion tensile strength property of the samples at varied percent copper addition

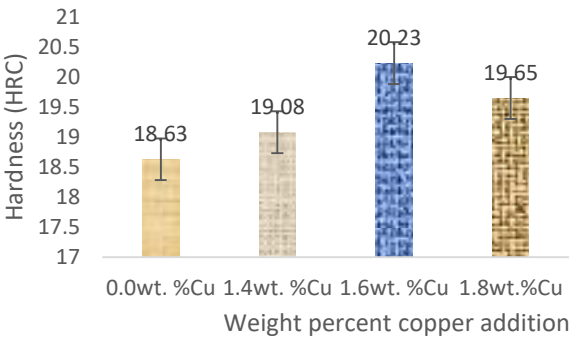

Figure 6: Post-corrosion hardness property of the samples at varied percent copper addition

CONCLUSIONS AND RECOMMENDATIONS

Based on the results work, the following conclusions were drawn:

i. Carbon equivalent values (CEVs) of control and 1.4wt. %, 1.6wt.% and 1.8wt.% copper alloyed samples, which are 3.15, 3.08, 3.10, and 3.17 respectively, Therefore, the samples are hypo-eutectic

ii. The pre-corrosion microstructures of the control GCI sample and copper alloyed GCI samples are heterogenous, comprising graphite flakes of varying sizes, and pearlite and ferrite of varied volume fraction. Graphite flakes of the control sample are thicker and sparsely distributed in the ferritic matrix. While graphite flakes of the copper alloyed samples are thin and densely distributed in pearritic- ferritic matrix.

iii. The highest tensile strength of 289 MPa and hardness of 20.96 HRC were revealed by the sample with 1.6 wt. %Cu addition, tensile strength of 286 Mpa, and hardness of 20.74 HRC were obtained upon further copper addition of 1.8 wt. %. Therefore, an optimum copper requirement was achieved at 1.6 wt. %Cu addition.

iv. Generally, corrosion-resistant characteristics of the copper alloyed samples were superior to the control sample, optimum corrosion rate of 0.06752 mmpy was revealed by the sample with 1.6 wt. % Cu addition, while the subsequent increase in copper addition of 1.8 wt. % led to an increase in the corrosion rate of 0.09593 mmpy.

v. Microstructures of the samples after corrosion were characterized by graphite flakes with varied volume fractions of ferrite and pearlite and the control sample revealed more susceptibility to corrosion attack.

vi. In comparison, the tensile strength and hardness properties of the samples after corrosion, which were 286 Mpa and 20.74 HRC respectively were lower than the corresponding tensile strength (289 Mpa) and hardness (20.96 HRC) before corrosion at the optimum copper addition of 1.6 wt.%.

REFERENCES

Adedayo, A. V. (2013). Relationship between graphite flake sizes and the mechanical properties of grey iron. *International Journal of Materials Science and Application*, 2(3), 94 - 98.

Agunsoye, J. O., Bello, S. A., Hassan, S. B., Adeyemo, R. G., & Odii, J. M. (2014). The effect of copper addition on the mechanical and wear properties of grey cast iron. *Journal of Minerals and Materials Characterization and Engineering*, 2, 470 - 483.

Akimov, A. G., Khodan, A. N., & Vechkanov, V.N. (1981). Formation of stable oxide films on the surface of chromium-nickel steel in a coolant based on N_2O_4, *At Energy*, 51, 733 - 735.

American Standard for Testing and Measurement E3-11(2011). Standard guide for preparation of metallographic specimens, ASTM International, West Conshohocken, www.astm.org.

American standard for testing and measurement E8-04. (2008). Standard test methods for tension testing of metallic materials, ASTM International, West Conshohocken, www.astm.org.

American Standard for Testing and Measurement G36 (2014). Standard Guide for Preparation of Corrosion coupons, ASTM International, West Conshohocken, www.astm.org.

American Standard for Testing and Measurement G5 – 94 (2004). Standard reference test method for making potentiostatic and potentiodynamic anodic polarization measurements.

American standard for testing and measurement E384-11 (2011). Standard test method for micro indentation hardness of materials, ASTM International. West Conshohocken, www.astm.org.

Asadi, Z. S., & Melchers, R. E. (2017). Pitting corrosion of older underground cast iron pipes. *Corrosion Engineering Science Technology.* 52, 459–469.

Bates, C. E. (1984). Effects of alloy elements on the strength and microstructure of gray cast iron. *Transactions of the American Foundrymen's Society, 92*, 923 - 946.

Behnam, M. M. J., Davami, P., & Varahram, N. (2010). Effect of cooling rate on microstructure and mechanical properties of grey cast iron. *Materials Science and Engineering*, A528, (2), 583–588.

Collini, L., Nicoletto, G., & Konecna, R. (2008). Microstructure and mechanical properties of pearlitic grey cast iron. *Materials Science and Engineering*, A 488(1-2), 529 - 539.

Fateh, A., Aliofrhazraei, M., & Rezvanian, A. R. (2020). Study of the effect of solidification on graphite flakes microstructure and mechanical properties of an ASTM a-48 grey cast iron using steel molds. Songklanakarin *Journal of Science and Technology*, 32(6), 613-618.

Bruna, H., Allende-Seco, R., Artigas, A., Monsalve, A., Sánchez, C. (2024). Effect of copper and nickel content on the corrosion mechanisms in ferritic matrix gray cast irons under simulated marine environments. *Metals, 14* (696), 1 – 18. https://doi.org/10.3390/met14060696

Hsu, C. H., & Chen, M. L. (2010). Corrosion behaviour of nickel alloyed and austempered ductile irons in 3.5% sodium chloride. *Corrosion Science*, *58*, 2945–2949.

Kidao, (1970). Application of copper in automotive iron castings. *Copper in Cast Iron*, 13 - 18.

Koch, G., Varney, J., Thompson, N., Moghissi, O., Gould, M., & Prayer, J. (2016). International Measures of Prevention, Application and Economic Corrosion Technology, NACE, International Impact Park ten Place, Houston, TX, USA [Google Scholar].

Lina, F. K. (2018). The corrosion behavior and wear resistance of grey cast iron. *Kuta Journal of Engineering*, 118 -132.

Lunarska, E. (1996). Effect of graphite shape on the corrosion of grey cast iron in phosphoric acid. *Journal of Materials and Corrosion, 47* (10), 539 - 544.

Rana, A. M., Khan A., & Amjad. S. (2001). Microstructure evaluation in heat treated cast irons. *Journal of Research (Science)*, 12, 65 - 71.

Rundman, K. B., Parolini, J. R., & Moore, D. J. (2005). Relationship between tensile properties and matrix microstructure in austempered gray iron. *AFS Transactions*, 145, 51 - 55.

Ruscak, M., & Perng, T. P. (1995). Effect of ferrite on corrosion of Fe-Mn-Al alloys in sodium-chloride solution, *Corrosion*, *51* (10), 738–743.

Seidu, S. O. Owoeye, S. S., & Owoyemi, H. T. (2015). Assessing the effect of copper addition on

corrosion behavior of grey cast iron, *Leonardo Electronic Journal Practices and Technologies*, 49-58.

Sarkar, T., Bose, P. K., & Sutradhar, G. (2018). Mechanical and tribological characteristics of copper alloyed austempered gray cast iron (AGI), *Material Today Proceeding; 5*, 3664 - 3673.

Sazegaran, H., Teimoori, F., Rastegarian, H., & Naserian-Nik A.M (2021). Effects of aluminium and copper on the graphite morphology, microstructure and compressive properties of ductile iron. *Journal of Mining and Metallurgy, Section B*, 57 (1) 145-154.

Sefiu, A. B., Bolaji, H., & Adeyemo, R. G. (2014). The effect of copper addition on the mechanical and wear properties of grey cast iron, *Journal of Minerals and Materials Characterization and Engineering* 2(5), 470-483.

Seidu, S. O. (2014). Effect of compositional changes on the mechanical behavior of grey cast iron. *Journal of Metallurgical Engineering*. 3 (2), 92 – 95.

Seikh, A. H., Sarkar, A., Singh, J. K., Mohammed, S. M. A. K., Alharthi, N., Ghosh, M. (2019). Corrosion characteristics of copper-added austempered gray cast iron (AGCI). *Materials, 12,* (503), 1 – 17. https://doi.org/10.3390/ma12030503

Upadhyay, S., & Saxena, K. K. (2020). Effect of Cu and Mo addition on mechanical properties and microstructure of grey cast iron: An overview: *Materials Today: Proceeding*, 26 (2), 2462-2470.

Sherrif, O. S., Saliu, O. S., Taiwo, S. A., & Lulian, R. (2019). Chilling effect of iron powder on the microstructure and hardness property of strongly hyper-eutectic grey cast iron. *ANNALS of Faculty Engineering Hunedaora, International Journal of Engineering*, 4, 13-22.

Stan, S., Chisamera, M., Riposan, I., Stefan, E., & Barstow, M. (2010). Solidification pattern of un-inoculated and inoculated gray cast irons in wedge test samples. *Transactions of the American Foundry Association (AFS), 118*, 295-309.

Tel'manova, O. N., Karyazin, P. P., & Shtanko, V. M. (2012). Behavior of cast-iron with lamellar and globular graphite in dilute acids. *Protection of Metals,6* (1), 45 - 47.

Vadiraj, A., & Tiwari, S. (2014). Effect of silicon on mechanical and wear properties of alloyed grey cast iron. *Journal of Materials Engineering and Performance*, 23, 3001-3006.

Xu, W., Ferry, M., & Wang, Y. (2005). Influence of alloying elements on as-cast microstructure and strength of grey iron. *Materials Science and Engineering A, 390*, 326 - 333.